Modeling individual and pairs of adsorbed polymer-grafted nanoparticles: structure and entanglements

Jeffrey G. Ethier and Lisa M. Hall*

William G. Lowrie Department of Chemical and Biomolecular Engineering, The Ohio State University, Columbus, Ohio 43210, United States

E-mail: hall.1004@osu.edu

Supporting Information Available

The end-to-end vector autocorrelation function ($\mathrm{ACF_{ee}}$) was calculated from

$$\mathrm{ACF_{ee}} = \frac{\left\langle \mathbf{R}_{\mathrm{ee}}(t) \cdot \mathbf{R}_{\mathrm{ee}}(0) \right\rangle}{\left\langle \mathrm{R}_{\mathrm{ee}}^2 \right\rangle} \tag{S1}$$

where $\mathbf{R}_{\mathrm{ee}}$ is the end-to-end vector of a polymer chain. The function was calculated for time blocks of $21,300\tau$ with starting times spaced 5243τ apart for short chain systems, and time blocks of $194,642\tau$ with starting times spaced 5243 apart for long chain systems. These block averaged functions were then averaged over the 4 trials with different starting configurations of the PGN. The autocorrelation function was then fit to a stretched exponential equation of the form $e^{-(\frac{t}{\tau})^{\beta}}$ using a least-squares fit. The least-squares fit was only applied up to two data points past the time at which $\mathrm{ACF_{ee}}$ decayed to $\frac{1}{e}$. We note that past this value, the autocorrelation function does not completely decorrelate or may have a multi-step relaxation, most likely due to particle rotation. Additionally, for PGN3-160, the statistical error was

larger since the average includes fewer polymer chains. We equilibrated our PGN systems well past the relaxation times to ensure proper equilibration.

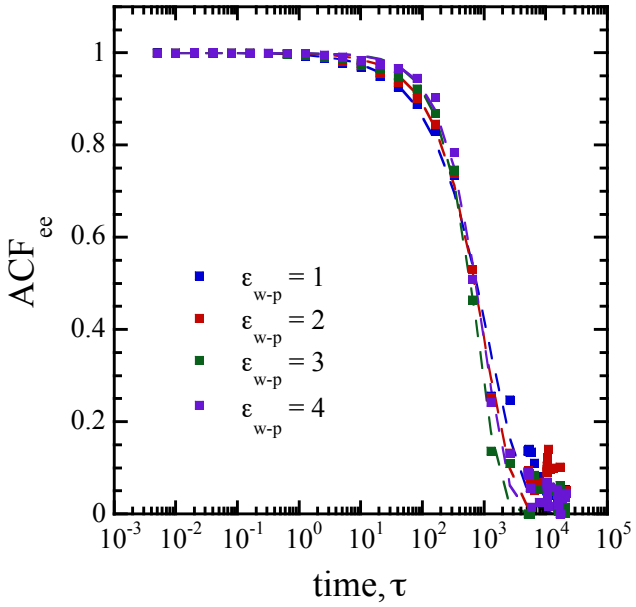

Figure S.1: End-to-end autocorrelation function (ACF_{ee}) for PGN6-35. Dashed lines are the stretched exponential fits.

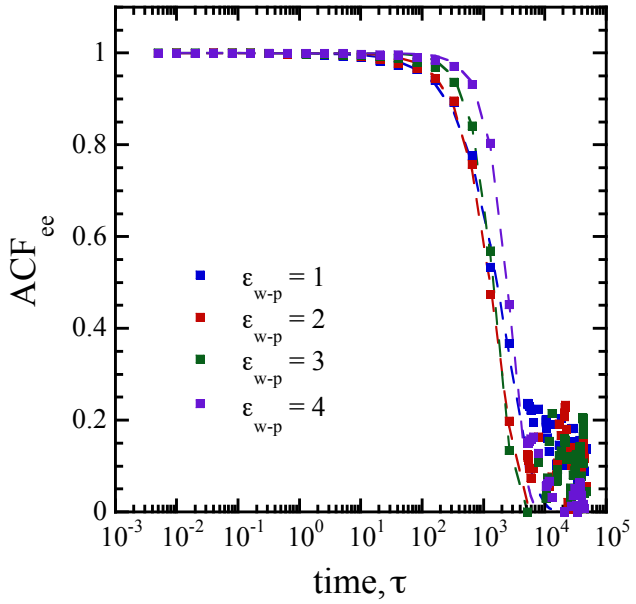

Figure S.2: End-to-end autocorrelation function (ACF_{ee}) for PGN3-160. Dashed lines are the stretched exponential fits.

The average number of nearest neighbors, $n(r_1)$, was calculated by integrating the monomer-

monomer radial distribution function from 0 to r_1, the local minimum located after the first peak. The number of nearest neighbors for the bulk melt is 12.4. The small decrease in the average number at the low adsorption strengths is due to the presence of the nanoparticle, vacuum, and wall. At the highest adsorption strength, the number of nearest neighbors decreases significantly, indicating that monomers shed a large number of nearest neighbors to interact with the surface.

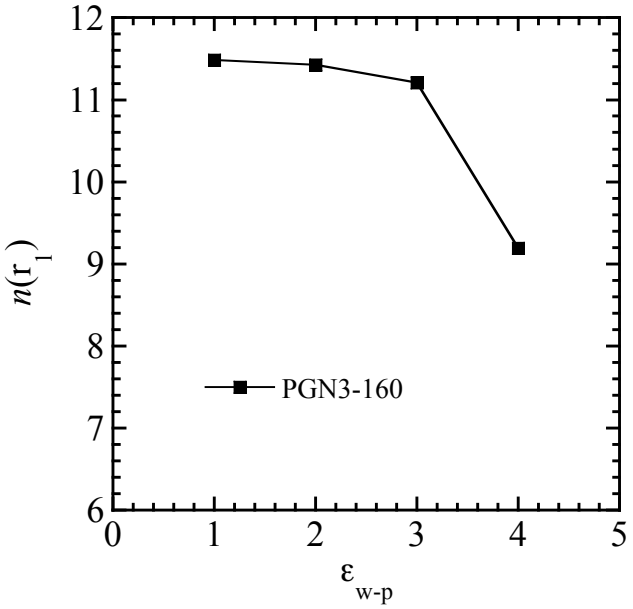

Figure S.3: Number of nearest neighbors, $n(\mathrm{r}_1)$ as a function of adsorption strength.

PGN6-35 and PGN3-160 particles were simulated without a surface (using shrink-wrapped boundary conditions) and their NP-monomer radial distribution functions are shown in Figure S.4. The NP-monomer $g(r)$ is compared with that of the lowest adsorption strength, $\epsilon_{\text{w-p}} = 1$. We find a slight change in the long-range part of $g(r)$, implying that the effect of the $\epsilon_{\text{w-p}} = 1$ surface on the canopy shape is small, especially for the short chain particle.

The distribution of end monomers for pairs of PGNs was calculated as a function of distance from the nanoparticle center (Figure S.5). These are histograms showing the number of a particle's grafted chains' ends within a particular spherical shell at distance r from the particle center with thickness $\delta r = 0.05$. Each distribution was normalized by the number of chains, N_{chains} and averaged over both particles.

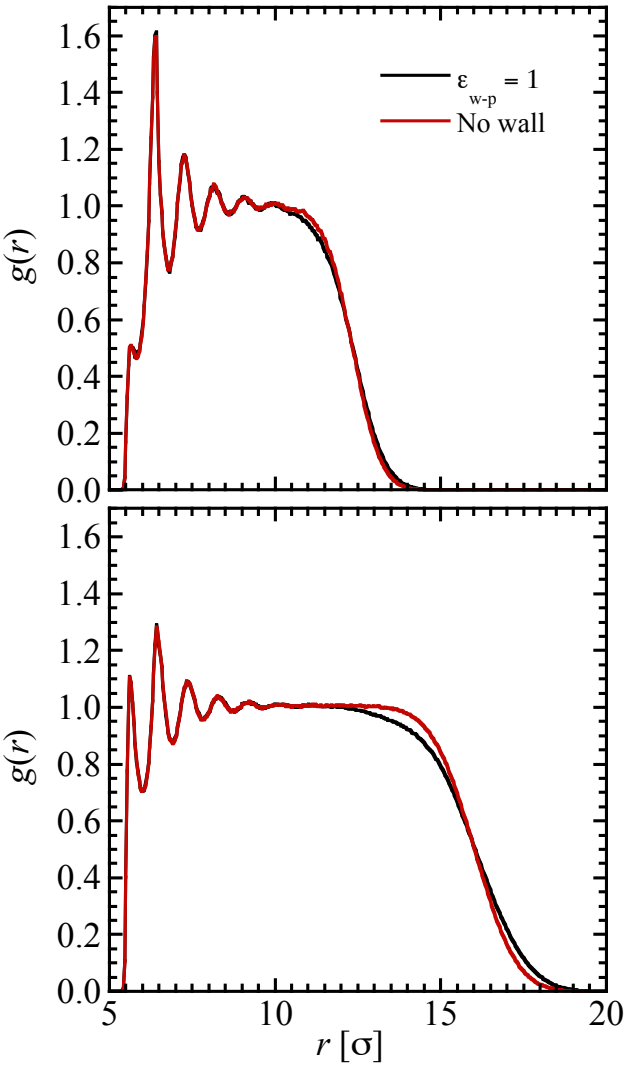

Figure S.4: Nanoparticle-monomer radial distribution function for PGN6-35 (top) and PGN3-160 (bottom) comparing the no wall profile with the lowest adsorption strength, $\epsilon_{\text{w-p}} = 1$.

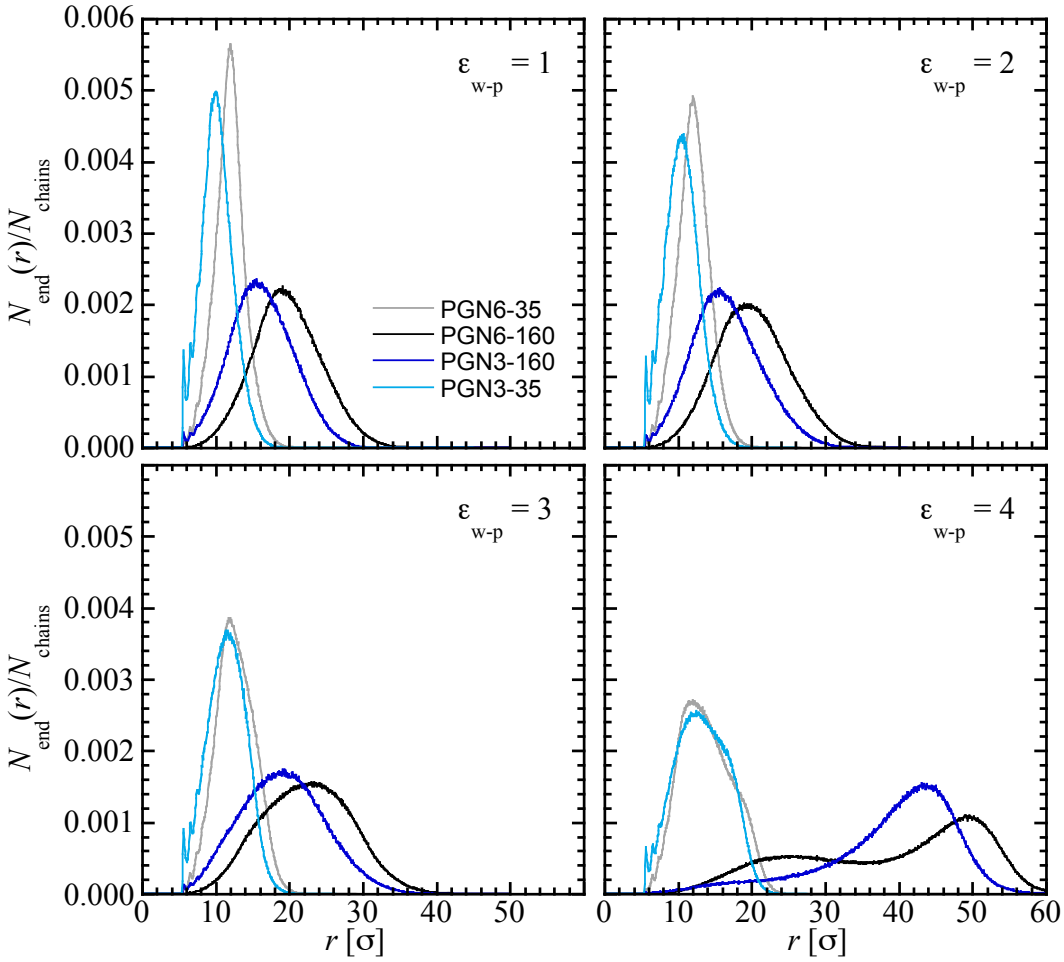

Figure S.5: Distribution of end monomers as a function of distance from the nanoparticle center and normalized by the number of chains. Each distribution is an average over the two particles in the simulation.